

Soft Matter

Accepted Manuscript



This is an *Accepted Manuscript*, which has been through the Royal Society of Chemistry peer review process and has been accepted for publication.

Accepted Manuscripts are published online shortly after acceptance, before technical editing, formatting and proof reading. Using this free service, authors can make their results available to the community, in citable form, before we publish the edited article. We will replace this *Accepted Manuscript* with the edited and formatted *Advance Article* as soon as it is available.

You can find more information about *Accepted Manuscripts* in the [Information for Authors](#).

Please note that technical editing may introduce minor changes to the text and/or graphics, which may alter content. The journal's standard [Terms & Conditions](#) and the [Ethical guidelines](#) still apply. In no event shall the Royal Society of Chemistry be held responsible for any errors or omissions in this *Accepted Manuscript* or any consequences arising from the use of any information it contains.

1 Title: Diffusion of macromolecules in self-assembled cellulose/hemicellulose hydrogels

2 Authors: Patricia Lopez-Sanchez¹, Erich Schuster^{2,3}, Dongjie Wang¹, Michael J Gidley¹, Anna Strom^{3,4}

3 ¹ ARC Centre of Excellence in Plant Cell Walls, Centre for Nutrition and Food Sciences, Queensland

4 Alliance for Agriculture and Food Innovation, The University of Queensland, Brisbane, 4072, Australia

5 ²Department of Structure and Material Design, The Swedish Institute for Food and Biotechnology,

6 SIK, Gothenburg, Sweden

7 ³SuMo BIOMATERIALS, VINN Excellence Center, Chalmers University of Technology, Gothenburg,

8 Sweden.

9 ⁴Applied Chemistry, Department of Chemical and Biological Engineering, Chalmers University of

10 Technology, Gothenburg, Sweden

11 Abstract

12 Cellulose hydrogels are extensively applied in many biotechnological fields and are also used as

13 models for plant cell walls. We synthesised model cellulosic hydrogels containing hemicelluloses, as

14 a biomimetic of plant cell walls, in order to study the role of hemicelluloses on their mass transport

15 properties. Microbial cellulose is able to self-assemble into composites when hemicelluloses, such as

16 xyloglucan and arabinoxylan, are present in the incubation media, leading to hydrogels with

17 different nano and microstructures. We investigated the diffusivities of a series of fluorescently

18 labelled dextrans, of different molecular weight, and proteins, including a plant pectin methyl

19 esterase (PME), using fluorescence recovery after photobleaching (FRAP). The presence of

20 xyloglucan, known to be able to crosslink cellulose fibres, confirmed by scanning electron

21 microscopy (SEM) and ¹³C NMR, reduced mobility of macromolecules of molecular weight higher

22 than 10kDa, reflected in lower diffusion coefficients. Furthermore PME diffusion was reduced in

23 composites containing xyloglucan, despite the lack of a particular binding motif in PME for this

24 polysaccharide, suggesting possible non-specific interactions between PME and this hemicellulose.
25 In contrast, hydrogels containing arabinoxylan coating cellulose fibres showed enhanced diffusivity
26 of the molecules studied. The different diffusivities were related to the architectural features found
27 in the composites as a function of polysaccharide composition. Our results show the effect of model
28 hemicelluloses in the mass transport properties of cellulose networks in highly hydrated
29 environments relevant to understanding the role of hemicelluloses in the permeability of plant cell
30 walls and aiding design of plant based materials with tailored properties.

31

32 Introduction

33 The architecture of the plant cell wall is directly related to its porosity and the transport of water
34 and molecules in the apoplast, the space outside of the cell membrane. Despite being of crucial
35 relevance to understand many biological and industrial processes, little is known about the complex
36 structural organisation and spatial distribution of plant cell wall polysaccharides and their
37 involvement in controlling the porosity and mass transport properties of the cell wall.¹ Although the
38 plant cell wall is permeable to water and low molecular weight compounds, it has limited
39 permeability for larger molecules e.g. enzymes and proteins involved in many bioprocesses such as
40 intercellular communication, growth and biomass conversions.

41 The plant cell wall of higher plants is proposed to be a double network of interacting but separated
42 networks of cellulose/hemicelluloses embedded in a pectin network, with generally minor amounts
43 of structural proteins such as extensins.² Due to the complexity of the cell wall, the role of individual
44 polysaccharides in controlling porosity and permeability is still not well understood, partly due to the
45 complexity of studying these properties *in planta*. Cellulose composites produced by the bacterium
46 *Gluconacetobacter xylinus* can be used as a simplified model of the plant cell wall while complexity is
47 added by the incorporation of different hemicelluloses and pectin.³⁻⁵

48 In the primary walls of dicots (and non-grass monocots) pectin, a complex biopolymer composed of
49 different polysaccharides such as homogalacturonan (HG), rhamnogalacturonan I (RG-I) and
50 substituted galacturonans like rhamnogalacturonan II (RG-II), is believed to determine wall porosity
51 creating the network with the smallest pores. Indeed it has been shown that after using pectinase
52 larger molecules could be transported, something that was not observed after the use of cellulase
53 and proteinase; suggesting that pectin controlled the porosity of the wall.⁶ Homogalacturonan in the
54 wall can be crosslinked with calcium creating a porous network, therefore parameters such as pH
55 and calcium concentration could be used to control the wall porosity by modifying the properties of
56 the pectin network.⁷ Furthermore the sugar side chains of branched RG-I, mainly arabinan and
57 galactan, have been proposed to play a role in controlling wall porosity.⁸

58 The role of hemicelluloses in the permeability of the cell wall has been less investigated and only
59 recently due to the interest from biofuel production to access cellulose in secondary thickened walls
60 e.g. characteristic of wood. Enzymatic degradation of plant cell walls is the most energy efficient
61 route to exploit plant biomass for energy or feed purposes.⁹ Plant cell walls are however, recalcitrant
62 to degradation by enzymes due to the intermolecular forces between polysaccharide components,
63 such as hemicelluloses and pectin. As for pectin, the presence of hemicelluloses is known to affect
64 the porosity of the cell wall of crops as removal of the hemicelluloses increased the pore size.¹⁰ Two
65 major kinds of hemicelluloses are xyloglucans and xylans. Xyloglucan is composed of a cellulose-like
66 backbone of β -(1-4)-linked-D-glucose branched by α -D-xylose molecules which can be further
67 substituted.¹¹ Xyloglucan in plants is found partially covering the cellulose microfibrils, entrapped
68 within some cellulose microfibrils and a minor but structurally highly relevant fraction includes the
69 parts of xyloglucans that crosslink cellulose microfibrils.¹² These crosslinks maintain the spaces
70 between cellulose microfibrils and are modulated by xyloglucan endo-transglycosylases and
71 expansins.^{13, 14} An example of xylans is arabinoxylan which has been identified in most cereal
72 endosperms. Arabinoxylan is a linear polymer of xylose molecules substituted at O-3 and/or O-2 by
73 arabinose residues, furthermore phenolics such as ferulic acid have been found esterifying O-5 of

74 occasional arabinose residues. Due to different extractabilities of arabinoxylan fractions, they are
75 claimed to interact in different ways in the plant cell wall: a water extractable weakly bound
76 fraction, held together by physical interactions and an alkali extractable tightly bound fraction, which
77 potentially is connected to other wall polysaccharides by ester-bond phenolic groups.

78 The diffusivity of molecules in the cell wall is influenced by the cell wall architecture, molecule-
79 molecule interactions and molecule-wall interactions which are different at different structural
80 length scales. Several methods are available to determine diffusion rates.¹⁵ The porosity and
81 molecule diffusion in the plant cell wall have been studied using ultrastructural methods such as
82 electron microscopy on isolated cell walls,¹⁶ bulk exclusion techniques¹⁷ on whole cells and
83 functional assays such as tracking molecules on whole cells under close to physiological conditions.¹⁸
84 However due to the differences intrinsic to the methods used and the heterogeneity of plant
85 materials a wide range of pore sizes, which can be related to cell wall permeability, have been
86 measured. Average pore sizes of 3.5-5.6 nm have been determined using bulk exclusion methods,
87 whereas functional assays suggest sizes of 4.5-9.2 nm. In general a continuous range of pore sizes
88 have been measured, abundant 4-5 nm pores which contribute to bulk uptake or exclusions and less
89 frequent 6-9 nm pores that allow larger molecules to penetrate more slowly.¹⁹

90 Fluorescence recovery after photobleaching (FRAP) in combination with confocal laser scanning
91 microscopy (CLSM) can be used to study molecular self-diffusion through heterogeneous materials.
92 FRAP offers the possibility to determine the diffusion rate locally and monitor the surrounding
93 structure simultaneously. In FRAP, the diffusion rate measurements are based on creating a
94 concentration gradient of fluorescent molecules. This is performed by deactivating the fluorescence
95 (photobleaching) in a region of interest (ROI) by exciting it using a high intensity laser beam. The
96 subsequent diffusion of the photo bleached molecules outside of the ROI and their replacement
97 with adjacent unbleached fluorochromes leads to a recovery of the fluorescence intensity. FRAP is
98 most useful for studying diffusion in the range of 0.1 to 100 $\mu\text{m}^2/\text{s}$ on a micrometer scale.^{20, 21} FRAP

99 has in the past been used to study the binding reversibility of cellulases to bacterial microcrystalline
100 cellulose fibrils and mats^{22, 23} as well as to study the mobility of labelled xylanases along the xylan
101 surface.²⁴ Using FRAP on soybean root cultured cells with fluorescently labelled dextrans and
102 proteins of graded size, a range of diameters for putative trans-wall channels was determined to be
103 6.6-8.6 nm.⁶ FRAP has also been used to study diffusion in pectin gels²⁵ and in feruloylated
104 arabinoxylan gels mixed with cellulose nanocrystals,²⁶ which served as plant cell wall models.

105 The determination of solute diffusion and molecular interactions is essential when investigating
106 diffusants with binding affinities and in biophysics,^{27, 28} since protein-protein interactions regulate
107 cellular processes. With an appropriate mathematical model, one can then analyze the fluorescence
108 recovery and extract quantitative information on the molecular dynamics. By considering a model
109 that contains an interaction term, it is possible to simultaneously estimate the pseudo-on binding
110 rate, the off binding rate, and the diffusion coefficient via FRAP.²⁷⁻³⁰

111 In this work we studied the role of hemicelluloses on the mass transport properties of cellulosic
112 hydrogels as a biomimetic of plant cell walls. Fluorescence recovery after photobleaching was used
113 in combination with confocal laser scanning microscopy to study molecular diffusion in cellulose
114 hydrogels (>95% water) and cellulose composite hydrogels containing xyloglucan or arabinoxylan,
115 selected as model hemicelluloses with different binding abilities to cellulose. A series of fluorescence
116 labelled dextrans and proteins of different molecular weights were used as models representative of
117 a range of plant molecules with different sizes. We also included a fluorescently labelled plant
118 methyl esterase (PME), selected for its lack of specificity to the hydrogel's components. Differences
119 in diffusion coefficients were attributed to microstructural changes introduced by the
120 hemicelluloses, characterised by SEM and ¹³C NMR. Our results revealed different effects of
121 hemicellulose in cellulose hydrogels and give insights into the potential contribution of different
122 polysaccharides to the permeability of the plant cell wall and man-made cellulose-based composites.

123

124 Experimental

125 Materials

126 Fluorescein isothiocyanate labelled dextran (FITC-dextran) of three different molecular weights
127 (10000 (FD 10), 70000 (FD 70), and 500000 (FD 500) g/mol) were purchased from Invitrogen
128 Molecular Probes, Eugene, OR. FITC labelled bovine serum albumin (FITC - BSA), orange pectin
129 methyl esterase (P5400 – 1KU with 154 units/mg solid or 597 units /mg protein), fluorescein 5(6)-
130 isothiocyanate (FITC, F7256), dimethyl sulfoxide (DMSO) and MES hydrate were purchased from
131 Sigma Aldrich, Steinheim, Germany. Dialysis membranes (Float-A-lyzer G2) with a Mw cut off size of
132 0.5-1 kDalton were obtained from SpectrumLabs, US.

133 Arabinoxylan extracted from wheat of a Mw of 370000 g/mol and xyloglucan extracted from
134 tamarind seed of a Mw of 225000 g/mol (both molecular weights are given by the supplier) were
135 purchased from Megazyme International Ltd, Ireland.

136 The Hestrin and Schramm medium used for incubation of the bacterial strain consisted of 1.15 g/l
137 citric acid (Ajax Finechem, Thermo Fisher Scientific, Australia), 2.7 g/l Na₂HPO₄ (Ajax Finechem,
138 Thermo Fisher Scientific, Australia), 5 g/l peptone (Oxoid LTD, Basingstoke, Hampshire, England), 5
139 g/l yeast extract (Becton, Dickinson and Company, Sparks, USA) and 2 % (w/v) glucose (Sigma-
140 Aldrich). The pH was adjusted to pH 5 with 10 M HCl.

141 Preparation of cellulose and cellulose/hemicellulose hydrogels

142 Xyloglucan and arabinoxylan solutions at a concentration of 1 % w/v were prepared by dissolving the
143 polysaccharides in deionised water overnight at room temperature.

144 The bacterial strain *Gluconacetobacter xylinus* (ATCC 53524 American Type Culture Collection,
145 Manassas, VA, USA) was used to produce cellulose (C), cellulose/xyloglucan (CXG) and
146 cellulose/arabinoxylan (CAX) hydrogels based on the method described by Chanliaud and co-

147 workers³ and Mikkelsen and co-workers³¹ with minor modifications. Hydrogels were cultivated in the
148 Hestrin and Schramm medium under static conditions at 30 °C. The cellulose/xyloglucan hydrogels
149 were produced by mixing the 1 % xyloglucan solution with double concentrated Hestrin and
150 Schramm medium (1:1) before inoculation, leading to a final xyloglucan concentration of 0.5 %. A
151 similar preparation method was used for the cellulose/arabinoxylan hydrogels. The samples were
152 harvested from the medium with forceps after 72 hours and washed 6 times with ice-cold deionised
153 water under agitation on an orbital platform shaker (KS 260 IKA-Werke, Staufen, Germany) at 150
154 rpm to dislodge the bacteria and remove excess medium.

155 All samples were disks with a diameter of approximately 40 mm, corresponding to the diameter of
156 the containers in which they were cultivated, and variable thickness of ca. 3 mm for C (cellulose), 2.2
157 mm for CAX (cellulose-arabinoxylan) and 0.3 mm for CXG (cellulose-xyloglucan). Samples were
158 stored in 0.02 % NaN₃ solution to avoid contamination and microbiological growth at 4 °C until
159 further analysis.

160 Methods

161 Concentration of cellulose hydrogels by compression

162 A mechanical tester machine, Instron 5565 A, was used to compress and concentrate the hydrogels
163 containing cellulose only (C). The samples were placed in the centre of the Instron platform and the
164 crosshead was lowered at a speed of 0.1 mm/s until a final thickness of 1 ± 0.1 mm was obtained, a
165 second set of samples was further compressed at 0.001 mm/s until a final thickness of 0.5 ± 0.1 mm
166 was reached.

167 Composites composition and microstructural characterisation

168 Dry weight measurements

169 Three samples of each type were dried in an oven at 105 °C for 24 h. The dry matter content was
170 calculated by weighing the samples in an analytical balance before and after drying.

171 Monosaccharide analysis

172 The degree of incorporation of hemicellulose in the hydrogels was analysed following the method by
173 Pettolino and co-workers³² with some variations. Compositions were calculated from individual
174 sugar contents on the basis of dry weights. Freeze dried samples (1-5 mg) were hydrolysed with 200
175 μl 12 M H_2SO_4 at 35 °C for 1 hour, diluted to 2 M using 3.5 ml water and incubated for a further 3
176 hours at 120 °C. The sample was cooled, then neutralised using approximately 550 μl of NH_4OH and
177 centrifuged at 2000 rpm for 10 minutes. An aliquot of 100 μl was collected; 5 μg of internal standard
178 (myo inositol) added and then dried with a stream of nitrogen. The sample was reduced using 200 μl
179 of 20 mg/ml sodium borodeuteride in DMSO at 40 °C for 90 min. The reductant was destroyed using
180 20 μl of acetic acid then acetylated by adding 25 μl 1-methylimidazol followed by 250 μl of acetic
181 anhydride. The sample was allowed to stand for 10 minutes, 2 ml of water was added followed by 1
182 ml dichloromethane (DCM) to extract the alditol acetates, the sample was mixed, centrifuged to aid
183 separation and the DCM phase was then washed twice with 2 ml of water. The DCM was then dried
184 under a stream of nitrogen and reconstituted into 100 μl of DCM, 1 μl of which was analysed by gas
185 chromatography attached to a mass spectrophotometer (GC-MS) using a high polarity BPX70
186 column.

187 Scanning electron microscopy (SEM)

188 Top and cross section images of the hydrogels were taken. Samples were freeze-substituted
189 according to the method of McKenna and co-workers³³ with minor modifications. At least 2 pieces of
190 each sample of approximately 1 cm^2 were quickly frozen in liquid nitrogen for 10 s, immediately
191 transferred to a container with 3 % glutaraldehyde in methanol at -20 °C and kept for 24 h. After that
192 the sample was transferred to another container with 100 % methanol at -20 °C for a further 24 h.

193 Samples were transferred to a microporous specimen capsule (120-200 μm , ProSci Tech, Thuringowa
194 QLD AUS) and immediately introduced into absolute ethanol solution at room temperature. For
195 cross section images, in house sample holders were fabricated that allow placing of the samples with
196 the cross section facing upwards in the direction of the electron beam. Samples were finally dried
197 using a Balzer critical point dryer (BAL-TEC AG, Liechtenstein). Dried samples were kept in a vacuum
198 desiccator at 40 °C overnight followed by plasma clean for 30 seconds (E.A.Fishione Plasma Cleaner,
199 PA, USA). Samples were then coated with iridium three times, from the top and from each side, at
200 10 mA for 100 s (Baltec Med 020 Platinum Coater, Switzerland) and kept in a vacuum desiccator until
201 microscopic observations. SEM micrographs were recorded using a JSM 7100F electron microscope
202 (JEOL, Japan) under the following conditions: accelerator voltage 5 kV, spotsize 2 and a working
203 distance (WD) of around 10 mm. Images were taken from at least three different positions of each
204 sample and 3 images were taken from each position, with a magnification increasing from *1,000,
205 *5,000, *10,000, *25,000, *50,000. Image analysis was performed using Image J software.³⁴

206 Solid State NMR

207 ¹³C CP/MAS and SP/MAS NMR experiments were performed as described elsewhere.⁵ Briefly a 13C
208 frequency of 75.46 MHz on a Bruker MSL-300 spectrometer was used. Samples were blotted dry and
209 packed in a 4-mm diameter, cylindrical, PSZ rotor with a Kelf end cap. The rotor was spun at 5 kHz at
210 the magic angle (54.7°). The 90° pulse width was 5 μs and a contact time of 1 ms was used for all
211 samples with a recycle delay of 3 s. The spectral width was 38 kHz, acquisition time 50 ms, time
212 domain points 2 k, transform size 4 k and line broadening 50 Hz. At least 2400 scans were
213 accumulated for each spectrum. Spectra were referenced to external adamantane. Using single
214 pulse direct polarization (SP/MAS) the mobile components of the composite spectra were observed.
215 The recycle time was 60 s and 20 k spectra were accumulated.

216 Preparation of fluorescent probes

217 Orange pectin methyl esterase was labelled with fluorescein 5(6)-isothiocyanate with some
218 modification of the method described by Videcoq and co-workers.²⁵ The enzyme was dissolved at a
219 concentration of 1 % (w/w) in 10 mM MES buffer at pH 7. FITC was dissolved in a mixture composed
220 of DMSO and water in a volumetric ratio of 2 : 1 to give a final FITC concentration of 0.015 mg/ml
221 DMSO and water. PME solution was added to the FITC / DMSO and water solution to yield a final
222 molar ratio between FITC and PME of 5 according to

$$223 \quad n^{\text{FITC}} / n^{\text{PME}} = 5.$$

224 The solution was stirred for 5 hours at 4 °C. The mixture was then dialysed against milliQ water to
225 remove excess FITC for three days, followed by dialysis against MES buffer (10 mM) for one day. The
226 dialysis tube used had a M_w cut off of 0.5-1 kDalton (Float-A-lyzer G2).

227 The FITC-dextran probes were incorporated into the hydrogels by the addition of 200 ppm of each
228 probe to the solution in which the hydrogels were kept. Similarly composites were mixed with 500
229 ppm of FITC-BSA and FITC-PME. The containers were covered with aluminium foil and left overnight
230 at 5 °C in order to give enough time for the probes to be homogeneously distributed in the gels.

231 CLSM-FRAP protocol

232 The CLSM system used consists of a Leica SP2 AOBS (Heidelberg, Germany) utilizing a 20x, 0.5 NA
233 water objective, with the following settings: 256 x 256 pixels, zoom factor 4 (with a zoom-in during
234 bleaching), and 800 Hz, yielding a pixel size of 0.73 μm and an image acquisition rate of two images
235 per second. The FRAP images were stored as 12-bit TIFF-images. The 488 nm line of an argon laser
236 was used to excite the fluorescent probes. The beam expander was set to 1, which lowered the
237 effective NA to ~ 0.35 and yielded slightly better bleaching and a more cylindrical bleaching profile.
238 The bleached areas will be called ROI in this study and were 30 μm large discs (nominal radius $r_n \sim 15$
239 μm) at 100 μm into the sample. The measurement routine consisted of 20 prebleach images. To
240 obtain an initial bleaching depth of ~ 30 % of the prebleach intensity in the ROI, one to four bleach

241 images were taken depending on the sample. For every recovery, at least 50 frames were recorded.

242 The FRAP data were normalized by the prebleach fluorescence intensity.

243 The respective diffusion probes were dissolved in deionised water to yield 200/500 ppm solutions.

244 The free diffusion coefficients D_0 of the probes in the absence of cellulosic hydrogels were
245 determined at ambient temperature, 7 μl of the probe solutions were placed into secure-seal spacer
246 grids between two cover glass slides, and the FRAP measurements were carried out on such locked
247 samples.

248 As described above, to prepare the cellulosic hydrogels for FRAP measurements the samples were
249 soaked in the respective probe solutions overnight. An approx. 2 cm \times 2 cm sized sample was cut,
250 the surface that was in direct contact with the liquid medium during cellulose synthesis was
251 absorbed on a cover glass slid, then loaded on the microscope stage and FRAP measurements
252 carried out in the upright mode of the microscope at ambient temperature. At least 6 FRAP
253 measurements were performed on different spatial coordinates per sample. To test the
254 reproducibility every sample was remade at least once. All of the recorded recoveries were quick
255 enough to yield Gaussian intensity distributions in the initial recovery images within the bleached
256 area/ROI. Therefore the FRAP model called "most likelihood estimation for FRAP data with a
257 Gaussian starting profile"³⁵ is valid for evaluation of the data. A script provided by Jonasson *et al.*³⁵
258 was utilized to analyze the data within this framework in Matlab, Mathworks, U.S.A.

259 To additionally analyze FRAP data for binding interactions, a quantitative approach to analyze
260 binding-diffusion kinetics by confocal FRAP was developed by Kang and co-workers,²⁹ and a data
261 analysis was carried out as described in³⁰.

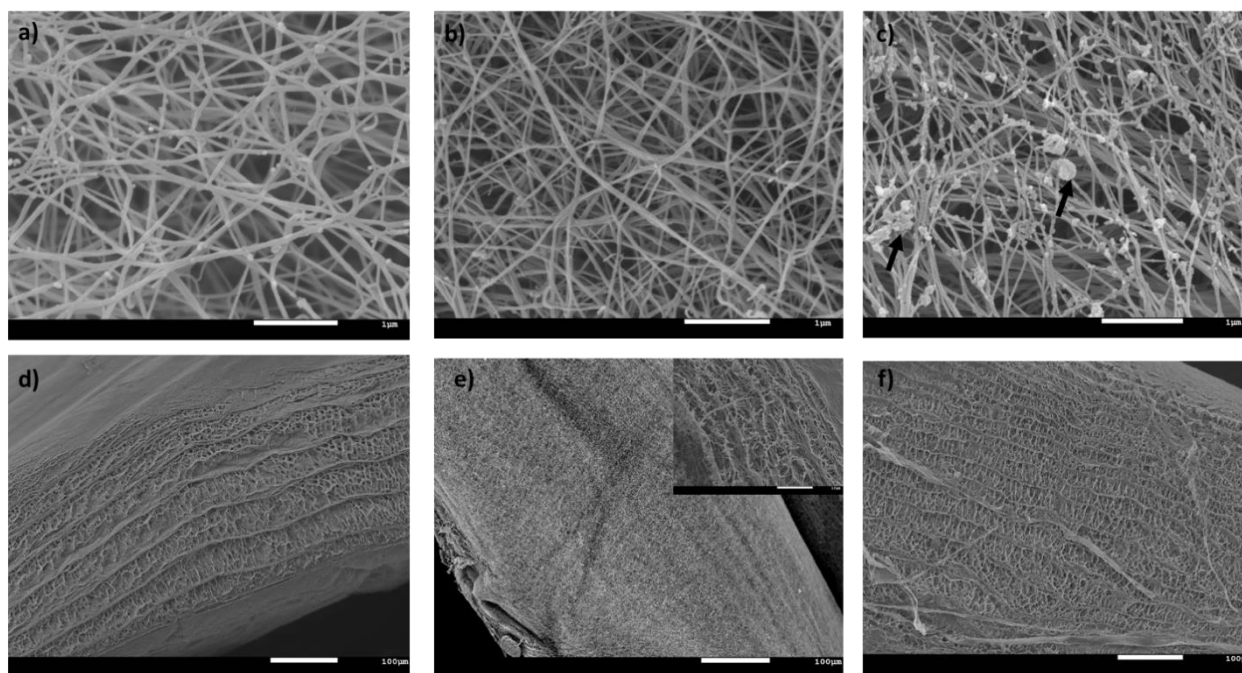
262 Results and discussion

263 Chemical and microstructural characterisation of cellulose/hemicellulose hydrogels

264 Chemical analysis of the composites by GC-MS confirmed an average incorporation of 40 % of
265 xyloglucan and 41.2 % arabinoxylan in the cellulose hydrogels. The average polysaccharide content
266 in the hydrogels was 1.3 % w/w for C, 1.5 % w/w for CAX and 2.5 % w/w in CXG. The cellulose
267 concentration was 1.3 % w/w for C, 0.9 % w/w for CAX and 1.5 % w/w for CXG. Furthermore the
268 presence of xyloglucan decreased the cellulose crystalline content from 87 % to 64 % (with the
269 percentage of I β allomorph increasing), arabinoxylan did not change the ratio crystalline:amorphous
270 compared to cellulose only samples, in agreement with previously reported data on similar
271 materials.⁵

272 A fraction of xyloglucan immobilised in the presence of cellulose was detected by ¹³C CP/MAS NMR
273 with a peak at 99.5 ppm due to the C1 of xylose (other xyloglucan C-1 signals are coincident with the
274 main cellulose C1 signal), and a mobile fraction was shown by a ¹³C SP/MAS spectrum attributable to
275 xyloglucan and not cellulose.³⁶ This behaviour is consistent with the crosslinks which could be
276 visualised under SEM as thin strands between cellulose fibres, although the higher density of these
277 composites made it difficult to identify different structural attributes (Figure 1b). In the
278 cellulose/arabinoxylan hydrogels, aggregates of different sizes were observed deposited on the
279 surface of the cellulose fibres (Figure 1c). These structures are attributed to aggregates of
280 arabinoxylan.³⁷ Arabinoxylan was still present after extensive washing of the samples suggesting that
281 arabinoxylan was interacting directly with the cellulose fibres. The ¹³C SP/MAS of arabinoxylan
282 composites revealed 2 peaks in the C1 region typical of arabinoxylan: xylose at 99.5 ppm and
283 arabinose at 104.2 ppm, but only cellulose signals were observed in the CP/MAS spectrum indicating
284 that arabinoxylan is present in the sample but it is not immobilised on the cellulose scaffold. These
285 features of the hydrogels have been previously reported.^{3, 5, 37} In the absence of hemicelluloses,
286 bacterial cellulose appeared as a mat of entangled long random oriented cellulose fibres with an
287 average diameter of 75 \pm 17 nm estimated from image analysis (Figure 1a). Similar cellulose
288 networks to the ones reported here after washing have been shown for unwashed pellicles³⁸,
289 confirming that the speed used in the rotational shaker is not enough to disturbed the tough

290 cellulose-hemicellulose networks. It should also be mentioned that the microstructure of the
 291 cellulose hydrogels remains unchanged at a compression speed of 0.1 mm/s compared to
 292 uncompressed samples whereas at 0.001 mm/s the cellulose fibres aggregate resulting in a
 293 densification of the structure.³⁹



294
 295 Fig. 1 Scanning electron micrographs of top and cross sections of cellulose only a) and d),
 296 cellulose/xyloglucan b) and e) and cellulose/arabinoxylan c) and f) composites. The magnification bar
 297 represents 1 μ m in the case of top images (a,b and c) and 100 μ m for the cross sections (d, e and f).
 298 The arrows indicate arabinoxylan aggregates.

299
 300 Cross section images of the hydrogels revealed a layer by layer structure in which the layers were
 301 connected by fibres of different lengths, giving rise to a broad range of pore sizes. This
 302 microstructure is the result of the way bacteria produce cellulose under these experimental
 303 conditions;⁴⁰ interestingly the average distance between the layers varied depending on the
 304 hydrogels composition. While the cellulose-only hydrogels had an average distance of $7.7 \pm 0.9 \mu\text{m}$
 305 (analysis of 11 images at different magnifications), the distance was increased to $10.7 \pm 2 \mu\text{m}$ when

306 arabinoxylan was present and reduced to $2.8 \pm 0.7 \mu\text{m}$ in the presence of xyloglucan. Although these
 307 overall numbers should be treated with caution since they could be influenced by sample
 308 preparation for SEM, the trends were clear with distances $\text{CAX} > \text{C} > \text{CXG}$.

309

310 FRAP measurements of probes in solution

311 The free diffusion coefficients D_0 of the probes in the absence of cellulosic hydrogels were
 312 determined at ambient temperature. This data yields hydrodynamic radii (r_H) – calculated using the
 313 Stokes–Einstein relation – and is displayed in Table 1. Additionally, the diffusion rate of the probes in
 314 solution is used later to calculate the normalized diffusivity D/D_0 , which indicates the degree of
 315 physical hindrance a probe within a hydrogel (diffusion rate D) encounters.

316 Table 1: Hydrodynamic radius and D_0 of the diffusion probes

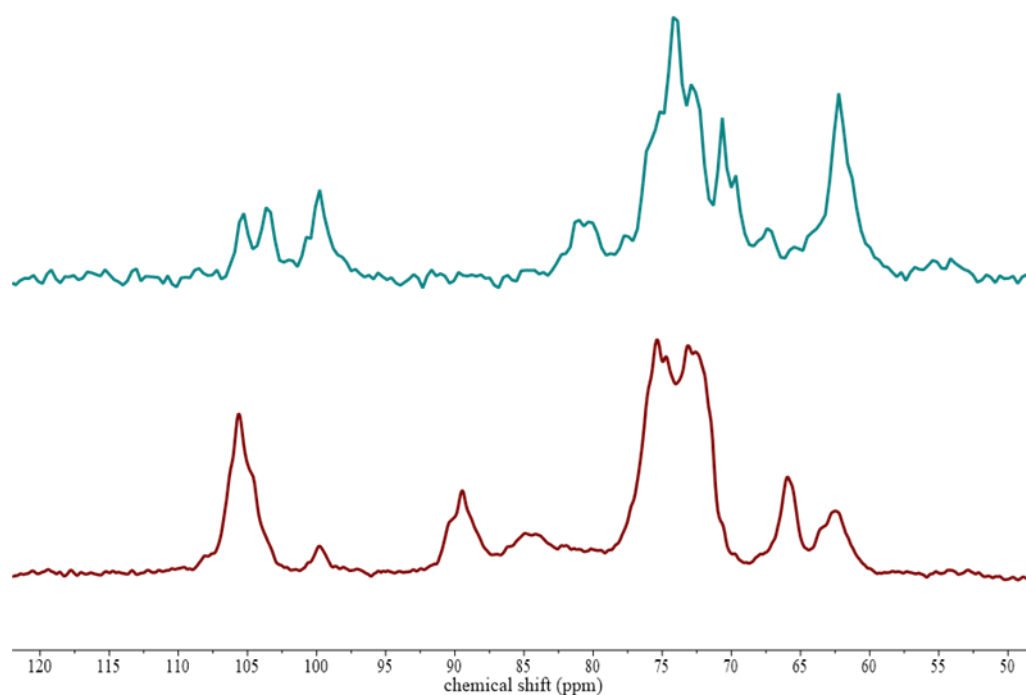
	r_H [nm]	D_0 [$\mu\text{m}^2/\text{s}$]
FITC dextran 10kDa	2.9 ± 0.3	82.8 ± 7.8
FITC dextran 70kDa	8.0 ± 0.5	30.0 ± 1.8
FITC dextran 500kDa	13.5 ± 1.1	17.8 ± 1.4
FITC albumin	4.7 ± 0.4	51.1 ± 4.0
FITC PME	1.2 ± 0.2	200 ± 35

317

318 To identify possible interactions of the probes with the hydrogel components, which might be
 319 responsible for their hindrance, ^{13}C NMR was carried out on composites which were soaked in
 320 500000 g/mol FITC-dextran solutions. ^{13}C SP/MAS and ^{13}C CP /MAS NMR spectra of
 321 cellulose/xyloglucan and cellulose/arabinoxylan soaked in FITC-dextran solutions were similar to
 322 those previously reported for these systems in the absence of dextran.⁵ Dextran is present in very
 323 low concentrations in the hydrogels compared to cellulose and xyloglucan or arabinoxylan, therefore

324 it was not possible to detect dextran in the ^{13}C NMR. Literature spectra show only one peak for
325 dextran between 60 and 70 and a C-1 signal at 100.5 ppm, which may be contributing to the larger
326 than expected xylose C-1 signal (Figure 2).

327



328

329 Fig. 2 ^{13}C SP/MAS and ^{13}C CP /MAS NMR spectra of cellulose/xyloglucan hydrogels soaked in a
330 500000 g/mol FITC-dextran solution. ^{13}C SP/MAS (top) ^{13}C CP/MAS (bottom).

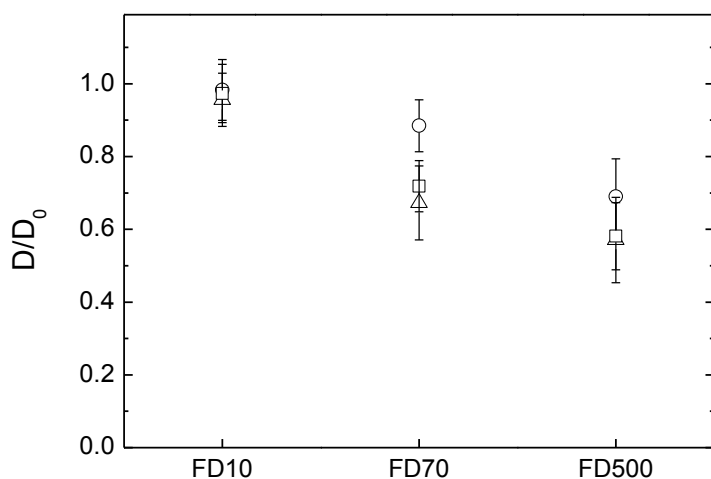
331

332 Probe diffusion in cellulose only hydrogels

333 The diffusion of probes in cellulose-only hydrogels was studied as a function of cellulose
334 concentration. Samples were compressed to different thicknesses; during compression water is
335 released radially from the hydrogels increasing the cellulose concentration. The cellulose
336 concentration of compressed samples can be estimated using the wet and dry weight and adjusting
337 for the volume of water loss.³⁹ Uncompressed cellulose samples had a thickness of 3 mm and a

338 concentration of 1.3 % w/w cellulose. Samples compressed at 0.1 mm/s to a final thickness of 1 ± 0.1
339 mm had a cellulose concentration of 3.9 %. It has been earlier reported³⁹ that the microstructure, in
340 terms of fibre diameter and pore size, of cellulose hydrogels compressed at rates of 0.1 mm/s was
341 very similar to that of uncompressed samples, however lower compression rates induced cellulose
342 fibre aggregation and increased the apparent pore size of the hydrogels. To further investigate the
343 effect of these structural changes on macromolecules diffusion, a second set of samples were
344 compressed at 0.001 mm/s to a thickness of 0.5 ± 0.1 mm, the final concentration of these samples
345 was 7.8 % w/w cellulose.

346 The diffusion of 10000 g/mol FITC - dextran in these different cellulose hydrogels was very similar
347 with D/D_0 close to 1, indicating that the probe moved freely in the structure. The D/D_0 of 70000
348 g/mol and 500000 g/mol dextran probes, was however slowed down in the uncompressed and 1
349 mm hydrogels compared to the 0.5 mm. The cellulose content of these samples increases from 1.3
350 to 7.8 % upon compression and the result of less hindered diffusion in the sample with higher
351 cellulose content may appear counter intuitive. However the cellulose fibres aggregate in the sample
352 with the higher amount of cellulose³⁹, thus potentially increasing the pore size of these hydrogels
353 and hence cause less obstruction for the diffusion probes. Alternatively the dynamic movements of
354 the fibres might have been reduced after aggregation and therefore reduced a barrier to diffusion
355 beyond static pore size effects. As would be expected, the diffusion of the probes are increasingly
356 hindered by the cellulose network as their molecular weight increases and thus their radius of
357 hydration estimated to be 2.9 nm for the 10000 g/mol , 8 nm for 70000 g/mol and 13.5 nm for the
358 500000 g/mol dextran respectively (Figure 3).



359

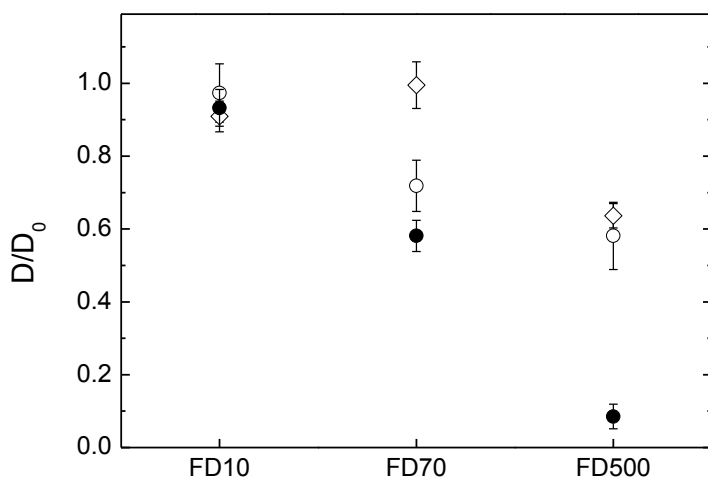
360 Fig. 3 Diffusion of FTIC-dextran molecules in three different cellulosic networks containing (Δ) 1.3 %
 361 cellulose (uncompressed \sim 3 mm), (\square) 3.9 % (compressed quickly to \sim 1 mm) and (\circ) 7.8 %
 362 (compressed slowly to \sim 0.5 mm)

363

364 Probe diffusion in cellulose/hemicellulose hydrogels

365 The diffusion in hydrogels containing both cellulose and hemicelluloses was compared with the
 366 cellulose-only hydrogels (Figure 4). As previously described, increasing the molecular weight and
 367 thus the radius of hydration of the dextran probes reduced their diffusivity in the pure cellulose
 368 hydrogels. The presence of arabinoxylan appears to increase the diffusivity of the dextran probes
 369 from the one observed in the cellulose-only hydrogels, especially for the 70000 g/mol FTIC- dextran.
 370 However, the presence of xyloglucan within the cellulose hydrogel reduced the diffusion of the
 371 70000 g/mol and the 500000 g/mol dextran considerably more compared to cellulose only. These
 372 results suggest in the case of cellulose / xyloglucan that the pore size was reduced compared to
 373 cellulose-only hydrogels. The observations made for the hydrogels where arabinoxylan was
 374 incorporated suggest either an increased pore structure, reduced dynamics of the network (not
 375 likely) or surface energy. The total polysaccharide content increased in the order cellulose <

376 cellulose/arabinoxylan < cellulose/xyloglucan, however the cellulose content was slightly lower in
377 the hydrogels containing arabinoxylan and higher in the hydrogels containing xyloglucan. The effect
378 of the hemicelluloses in the overall cellulose content of the hydrogels has an impact on
379 microstructural effects such as pore size distribution. Indeed, scanning electron micrographs of top
380 and cross sections indicated a denser network in the presence of xyloglucan compared to cellulose
381 only hydrogels furthermore, the distance between the observed fibre layers in the structure was
382 significantly reduced. This is expected for a molecule acting as a cross linker between cellulose fibres
383 which would bring cellulose fibres closer together and lead to increased density of the system. On
384 the other hand the presence of a molecule only interacting at the fibre surface, not crosslinking, as is
385 the case of arabinoxylan, led to a microstructure similar to cellulose only. The coating of
386 arabinoxylan on the cellulose fibre may instead render the arabinoxylan-containing network less
387 hydrophilic as the contact angle between water and washed arabinoxylan is higher (67-74°)⁴¹ than
388 cellulose (40°) and xyloglucan (20°)⁴². A change to a less hydrophilic network increases the mobility
389 of fluorescently labelled probes due to repulsion between the probe and the network, similar to
390 observations on systems in which electrostatic repulsion between the probe and the matrix
391 increased the mobility compared to a non-charged reference.⁴³ In principle, the same trend would
392 be expected for the 500000 Da probe, however the repulsion related to probe / network interaction
393 may here be overruled by the physical constraints of the network itself.



394

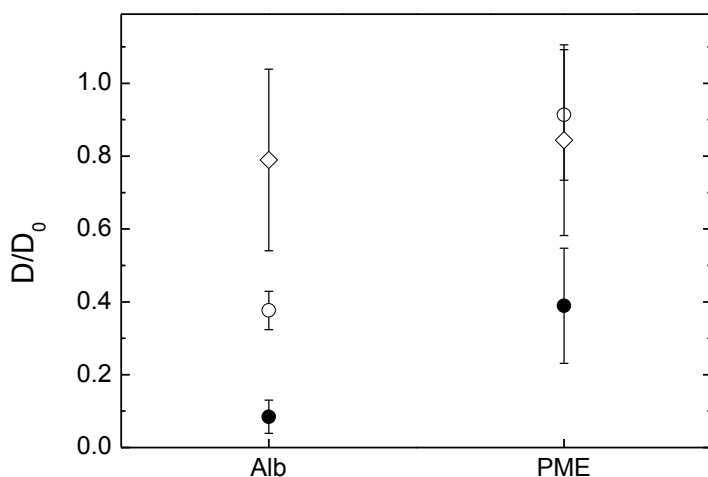
395 Fig. 4 Diffusion of FTIC-dextran molecules in three different hydrogels containing (○) cellulose only
 396 (1.8% compressed to 1 mm) (●) cellulose/xyloglucan and (◇) cellulose/arabinoxylan.

397 The diffusivity of the two charged probes, albumin and PME, differed depending on the network
 398 composition (Figure 5). It is worthwhile to mention that both albumin and PME can be
 399 approximately compared to the 10 000 g/mol dextran in size as their radius of hydration are close to
 400 4.7 and 1.2 nm respectively where the 10 000 g/mol dextran is of 2.9 nm in r_H . The diffusion of the
 401 albumin is less hindered in cellulose/arabinoxylan composite followed by the pure cellulose and
 402 nearly immobile in the composite sample containing xyloglucan. The hindrance of the albumin in the
 403 different composites (except for the cellulose/arabinoxylan) cannot only be explained by the pore
 404 size of the respective networks as the size of the albumin is similar to the size of the 10 000 g/mol
 405 dextran, which is less hindered. An anomalous diffusion i.e. slower diffusion than expected of bovine
 406 serum albumin as used in this study was observed also in arabinoxylan gels, prepared as model
 407 system for the secondary plant cell wall. In this study the authors concluded that the interaction
 408 observed most probably was related to some interaction between the albumin and the gel network
 409 itself²⁶ while other studies have observed hindrance of albumin in other polysaccharide solutions.⁴⁴

410 ⁴⁵ It is shown in this study that the albumin appears to interact even stronger with the cellulose and
411 cellulose/xyloglucan compared to the cellulose/arabinoxylan network.

412

413 In the case of PME, its diffusivity in pure cellulose and cellulose arabinoxylan were similar.
414 Furthermore, it was similar to the dextran of 10 kDa i.e., only slightly reduced by the network. This
415 was expected as PME has a rH of ~ 1 nm, thus too small to be hindered by the network studied here.
416 Surprisingly, the diffusivity of the PME was largely reduced in the cellulose/xyloglucan gel, more so
417 than 70 kDa dextran with a rH of ~ 8 nm. The hindrance of the PME in the cellulose/xyloglucan
418 sample can only be explained by additional interactions between the probe and the polysaccharide
419 matrix rather than hindrance related to pore size. In order to test the behaviour of PME in the
420 presence of xyloglucan and elaborate if there are any interactions which could permanently or
421 temporarily bind the PME, additional experiments on a 1 % w/w xyloglucan solution were carried
422 out. FRAP measurements were carried out on FITC-PME in the xyloglucan solution. The recovery
423 curve was analysed in the framework of FRAP and binding, and showed that in a 1 % w/w xyloglucan
424 solution PME's mobility is hindered around 20 % ($D/D_0 = 0.79 \pm 0.07$). Binding with pseudo-on
425 binding rate constant $k_{on}^* = 0.5 \pm 0.4 \text{ s}^{-1}$ and off binding rate constant one magnitude higher ranging
426 $k_{off} = 20 \pm 10 \text{ s}^{-1}$ indicates that transient interactions on a time-scale of 30 ms – 10 s are occurring and
427 a fraction of ~ 5 % of the PME are in average bound to the xyloglucan.



428

429 Fig. 5 FITC-albumin and FITC-PME diffusion in (○) cellulose only hydrogels (1.8% cellulose)

430 compressed to 1 mm, (●) cellulose/xyloglucan and (◇) cellulose/arabinoxylan hydrogels.

431

432 Our results indicate that PME interacts with xyloglucan in the composites: pectin methyl esterase is

433 an enzyme which de-esterifies methylgalacturonic acid esters in pectins, therefore no interaction

434 was expected with these composites which contain only cellulose and hemicelluloses. It is known

435 that cell wall polysaccharides interact with their specific enzymes by carbohydrate binding sites

436 outside of the active site area. These binding sites can be found on carbohydrate binding modules

437 (CBMs) which are independent domains or they can be present on the surface of enzymes on

438 catalytic domains or other intimately associated domains known as surface binding sites (SBSs) ⁴⁶.

439 Furthermore CBMs have been shown to improve the action of catalytic modules on polysaccharides

440 in plant cell walls through the recognition of non-substrate polysaccharides ¹. This function was

441 proved in a pectate lyase, whose degrading pectic homogalacturonan action was increased by

442 cellulose-directed CBMs but not by xylan-directed CBMs. Furthermore the activity of hemicellulosic

443 enzymes such as arabinofuranosidase, which removes side chains from arabinoxylan in xylan-rich

444 and cellulose-poor wheat grain endosperm cell walls, was enhanced by a xylan-binding CBM.

445 Examples in secondary cell walls have also been shown; xylanase degradation of xylan was
446 potentiated by both xylan and cellulose-directed CBMs.¹ We propose that PME can potentially have
447 CBM's which might aid the action of this enzyme during cell wall growth and development by
448 interacting with non-substrate polysaccharides such as xyloglucan. The primary plant cell wall is a
449 highly concentrated environment of polysaccharides where pectins and xyloglucans are in close
450 contact, therefore the possibility of enzymes using non substrates to improve their action seems
451 reasonable. Based on the diffusion results of PME in xyloglucan solutions this interaction cannot be
452 only steric but of physical/adhesive nature. Further work is required to characterise this interaction
453 between PME and xyloglucan.

454

455 Conclusions

456 Composition of cellulose-based hydrogels (cellulose, cellulose/arabinoxylan, cellulose/xyloglucan)
457 influence the diffusion of FITC labelled dextran at $r_h > 4\text{nm}$ and $M_w > 10\text{kDa}$ and protein probes even
458 at r_h as low as 1nm . Cellulose/xyloglucan hydrogels reduce the mobility of all probes to a larger
459 extent than cellulose and cellulose/arabinoxylan. The reduced mobility of the probes in the
460 cellulose/xyloglucan hydrogel can in the case of dextran be explained by change in microstructure.
461 The diffusion of fluorescently labelled PME was slightly reduced in the cellulose and the
462 cellulose/arabinoxylan gel but greatly reduced in the cellulose/xyloglucan hydrogel. An interaction
463 between PME and xyloglucan has to our knowledge not been reported previously. Our results
464 indicate the possibility of such an interaction, an observation which merits further investigation.
465 Using proteins as model probes for diverse enzymes does not give adequate information on its own
466 as it ignores specific interactions as shown by the fact that the mobility of e.g. PME was not reduced
467 in the presence of cellulose and arabinoxylan while albumin mobility was reduced in all networks.

468 Acknowledgements

469 Cherie T. Beahan is gratefully acknowledged for performing monosaccharide analysis on the
470 composites. Bernadine Flanagan is acknowledged for performing ^{13}C NMR experiments. The financial
471 support from VINN EXcellence SuMo Biomaterials (Supramolecular Biomaterials – Structure
472 dynamics and properties) to AS and ES as well as VINNMER to AS are acknowledged. This work was
473 carried out with the financial support of a UQ Start-up research grant to PLS.

474 References

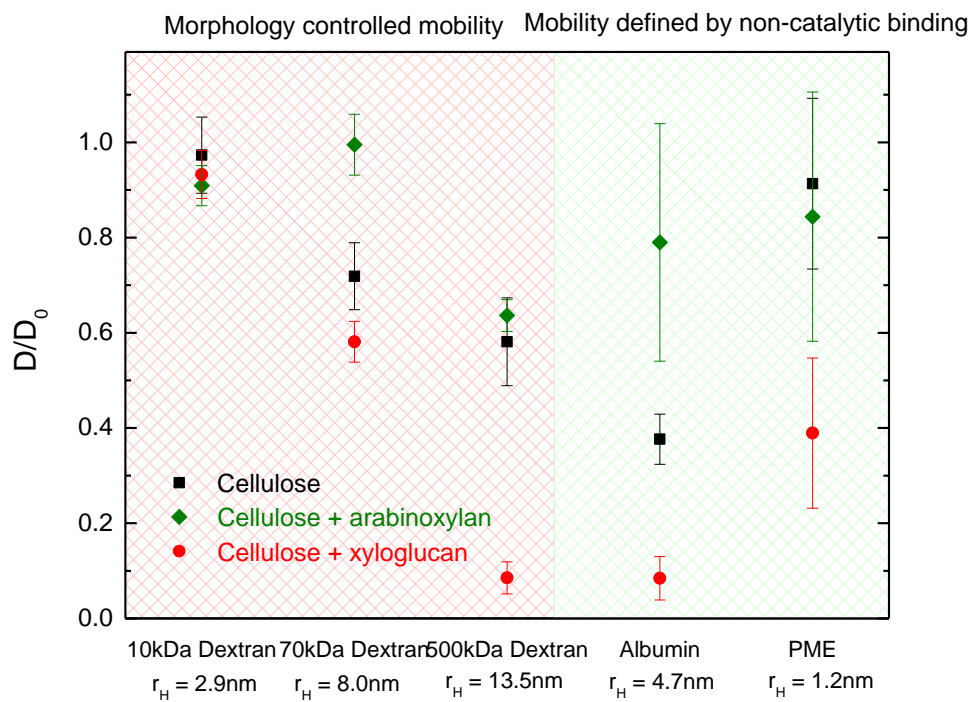
- 475 1. C. Herve, A. Rogowski, A. W. Blake, S. E. Marcus, H. J. Gilbert and J. P. Knox, *Proc. Natl. Acad.*
476 *Sci. U. S. A.*, 2010, **107**, 15293-15298.
- 477 2. Y. B. Park and D. J. Cosgrove, *Plant Physiol*, 2012, **158**, 1933-1943.
- 478 3. E. Chanliaud, K. M. Burrows, G. Jeronimidis and M. J. Gidley, *Planta*, 2002, **215**, 989-996.
- 479 4. S. E. C. Whitney, M. G. E. Gothard, J. T. Mitchell and M. J. Gidley, *Plant Physiol.*, 1999, **121**,
480 657-663.
- 481 5. P. Lopez-Sanchez, J. Cersosimo, D. Wang, B. Flanagan, J. R. Stokes and M. J. Gidley, *PLoS One*,
482 2015, **10**, e0122132.
- 483 6. O. Baronepel, P. K. Gharyal and M. Schindler, *Planta*, 1988, **175**, 389-395.
- 484 7. M. C. Jarvis, *Plant, Cell Environ.*, 1984, **7**, 153-164.
- 485 8. T. J. Foster, S. Ablett, M. C. McCann and M. J. Gidley, *Biopolymers*, 1996, **39**, 51-66.
- 486 9. M. Pauly and K. Keegstra, *Plant J.*, 2008, **54**, 559-568.
- 487 10. F. Adani, G. Papa, A. Schievano, G. Cardinale, G. D'Imporzano and F. Tambone, *Environ. Sci.*
488 *Technol.*, 2011, **45**, 1107-1113.
- 489 11. A. Ebringerova, Z. Hromadkova and T. Heinze, *Adv. Polym. Sci.*, 2005, **186**, 1-67.
- 490 12. M. Pauly, P. Albersheim, A. Darvill and W. S. York, *Plant J.*, 1999, **20**, 629-639.
- 491 13. M. C. McCann, B. Wells and K. Roberts, *J. Cell Sci.*, 1990, **96**, 323-334.
- 492 14. T. Fujino, Y. Sone, Y. Mitsuishi and T. Itoh, *Plant Cell Physiol.*, 2000, **41**, 486-494.
- 493 15. B. A. Westrin, A. Axelsson and G. Zacchi, *J. Controlled Release*, 1994, **30**, 189-199.
- 494 16. M. C. McCann, B. Wells and K. Roberts, *J. Cell Sci.*, 1990, **96**, 323-334.
- 495 17. M. Tepfer and I. E. P. Taylor, *Science*, 1981, **213**, 761-763.
- 496 18. A. B. Stephen M. Read, in *Modern methods of plant analysis. Plant cell analysis*, ed. H. F. L. a.
497 J. F. Jackson., Springer-Verlag Berlin Heilderberg, 1996, vol. 17.
- 498 19. M. A. Horn, P. F. Heinsteins and P. S. Low, *Plant Physiol.*, 1992, **98**, 673-679.
- 499 20. H. Deschout, J. Hagman, S. Fransson, J. Jonasson, M. Rudemo, N. Loren and K. Braeckmans,
500 *Optics Express*, 2010, **18**, 22886-22905.
- 501 21. E. Schuster, J. Eckardt, A. M. Hermansson, A. Larsson, N. Loren, A. Altskar and A. Strom, *Soft*
502 *Matter*, 2014, **10**, 357-366.
- 503 22. J. M. Moran-Mirabal, J. C. Bolewski and L. P. Walker, *Biophys. Chem.*, 2011, **155**, 20-28.
- 504 23. J. M. Moran-Mirabal, *Cellulose*, 2013, **20**, 2291-2309.
- 505 24. S. Cuyvers, J. Hendrix, E. Dornez, Y. Engelborghs, J. A. Delcour and C. M. Courtin, *J. Phys.*
506 *Chem. B*, 2011, **115**, 4810-4817.
- 507 25. P. Videcoq, K. Steenkeste, E. Bonnin and C. Garnier, *Soft Matter*, 2013, **9**, 5110-5118.
- 508 26. G. Paes and B. Chabbert, *Biomacromolecules*, 2012, **13**, 206-214.
- 509 27. B. L. Sprague, R. L. Pego, D. A. Stavreva and J. G. McNally, *Biophys. J.*, 2004, **86**, 3473-3495.
- 510 28. F. Mueller, D. Mazza, T. J. Stasevich and J. G. McNally, *Curr. Opin. Cell Biol.*, 2010, **22**, 403-
511 411.
- 512 29. M. C. Kang, C. A. Day, E. DiBenedetto and A. K. Kenworthy, *Biophys. J.*, 2010, **99**, 2737-2747.

- 513 30. E. Schuster, A. M. Hermansson, C. Ohgren, M. Rudemo and N. Loren, *Biophys. J.*, 2014, **106**,
514 253-262.
- 515 31. D. Mikkelsen and M. J. Gidley, in *Plant Cell Wall: Methods and Protocols*, ed. Z. A. Popper,
516 2011, vol. 715, pp. 197-208.
- 517 32. F. A. Pettolino, C. Walsh, G. B. Fincher and A. Bacic, *Nat. Protoc.*, 2012, **7**, 1590-1607.
- 518 33. B. A. McKenna, D. Mikkelsen, J. B. Wehr, M. J. Gidley and N. W. Menzies, *Cellulose*, 2009, **16**,
519 1047-1055.
- 520 34. C. A. Schneider, W. S. Rasband and K. W. Eliceiri, *Nat. Methods*, 2012, **9**, 671-675.
- 521 35. J. K. Jonasson, N. Loren, P. Olofsson, M. Nyden and M. Rudemo, *J. Microsc. (Oxford, U. K.)*,
522 2008, **232**, 260-269.
- 523 36. M. J. Gidley, P. J. Lillford, D. W. Rowlands, P. Lang, M. Dentini, V. Crescenzi, M. Edwards, C.
524 Fanutti and J. S. G. Reid, *Carbohydr. Res.*, 1991, **214**, 299-314.
- 525 37. D. Mikkelsen, M. J. Gidley and B. A. Williams, *J Agric Food Chem*, 2011, **59**, 4025-4032.
- 526 38. D. Lin, P. Lopez-Sanchez and M. J. Gidley, *Carbohydr. Polym.*, 2015,
527 doi:10.1016/j.carbpol.2015.1003.1048.
- 528 39. P. Lopez-Sanchez, M. Rincon, D. Wang, S. Brulhart, J. R. Stokes and M. J. Gidley,
529 *Biomacromolecules*, 2014, **15**, 2274-2284.
- 530 40. M. Y. Iguchi, S.; Budhiono, A., *J. Mater. Sci.*, 2000, **35**, 9.
- 531 41. I. Egues, A. M. Stepan, A. Eceiza, G. Toriz, P. Gatenholm and J. Labidi, *Carbohydr. Polym*,
532 2014, **102**, 12-20.
- 533 42. G. Raj, E. Balnois, M. A. Helias, C. Baley and Y. Grohens, *J. Mater. Sci.*, 2012, **47**, 2175-2181.
- 534 43. N. Fatin-Rouge, A. Milon, J. Buffle, R. R. Goulet and A. Tessier, *J. Phys. Chem. B*, 2003, **107**,
535 12126-12137.
- 536 44. T. C. Laurent and H. Persson, *Biochim. Biophys. Acta*, 1964, **83**, 141-&.
- 537 45. S. C. De Smedt, A. Lauwers, J. Demeester, Y. Engelborghs, G. Demey and M. Du,
538 *Macromolecules*, 1994, **27**, 141-146.
- 539 46. D. Cockburn, C. Wilkens, C. Ruzanski, S. Andersen, J. W. Nielsen, A. M. Smith, R. A. Field, M.
540 Willemoes, M. Abou Hachem and B. Svensson, *Biologia*, 2014, **69**, 705-712.

541

542

543



The different effects of hemicelluloses on the diffusion properties of cellulose hydrogels is related to architectural features.